Journal of
Water & Climate Change

IWA PUBLISHING

Journal of Water and Climate Change Vol 15 No 8, 4114 doi: 10.2166/wcc.2024.294

Spatiotemporal variation characteristics of precipitation and urbanization effects in Shenzhen from 1960 to 2019

Shouwei Shang[a,*], Yintang Wang[a], Xinyi Chen[b], Tingting Cui[a] and Chaofan Pan[a]

[a] State Key Laboratory of Hydrology-Water Resources and Hydraulic Engineering, Nanjing Hydraulic Research Institute, Nanjing 210029, China
[b] College of Hydrology and Water Resources, Hohai University, Nanjing 210098 China
*Corresponding author. E-mail: ssw971216@163.com

ABSTRACT

To explore the evolution of precipitation in megacities under changing environments and human activities, Shenzhen was chosen as the study area. Using daily precipitation data from 10 stations (1960–2019), the TFPW-MK and EOF methods analyzed the spatiotemporal characteristics of precipitation. The findings are: (a) Precipitation in Shenzhen shows a slight upward trend with spatial variations. Western stations exhibit a downward trend. The oscillation period of precipitation indicators is about 10–20 years, with an abrupt change in 1991. (b) Different precipitation indicators have similar distribution patterns. The first mode shows global consistency, indicating overall high or low precipitation, and a shift in the precipitation center from northwest (before 1990) to southeast (after 1990). The second mode shows an "East-West" reverse distribution. (c) Urbanization significantly affects precipitation distribution and has an enhancing effect on precipitation. The smaller the time scale, the stronger the effect of urbanization on extreme precipitation.

Key words: empirical orthogonal function, extreme precipitation, precipitation, Shenzhen, spatiotemporal evolution, trend

HIGHLIGHTS

- The precipitation changes were analyzed from multiple scales.
- The TFPW-MK and EOF methods were used to analyze the spatiotemporal changes of precipitation and found that the precipitation center changed from the southeast to the northwest.
- Urbanization has a certain rainfall-enhancing effect on precipitation. The smaller the precipitation scale, the stronger the rainfall-enhancing effect of urbanization.

GRAPHICAL ABSTRACT

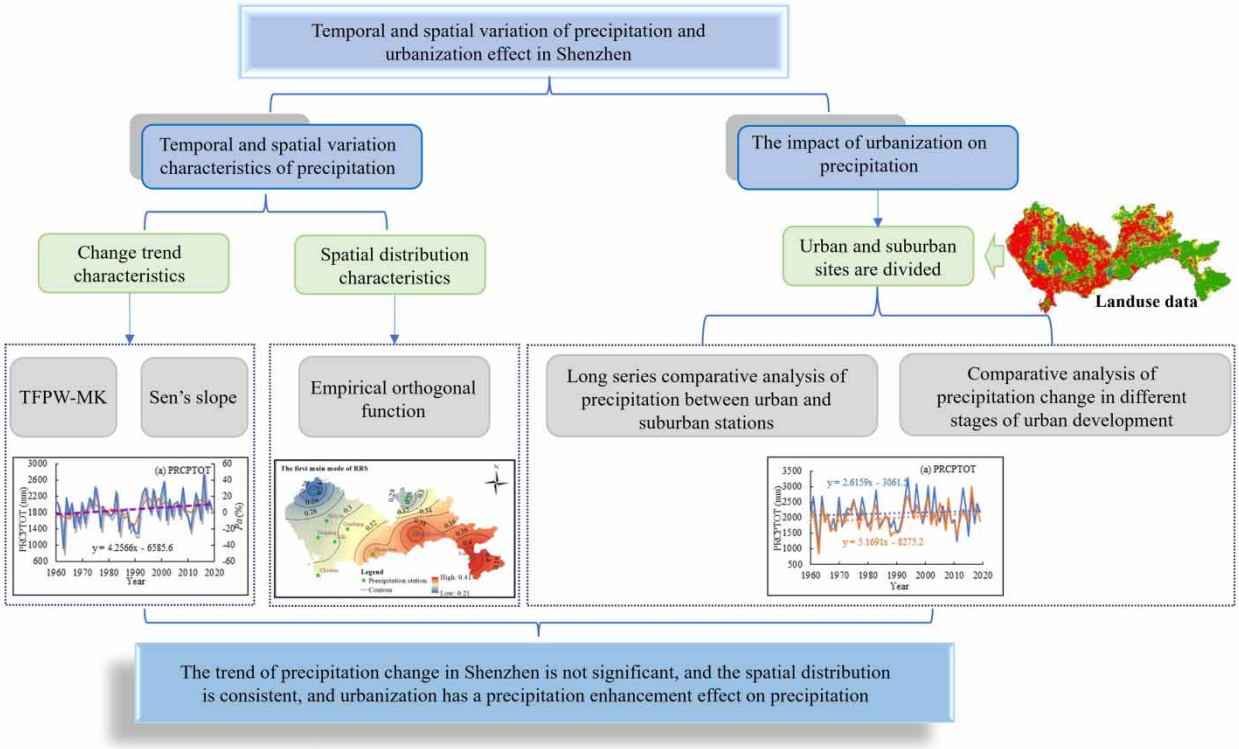

1. INTRODUCTION

Under the dual influence of climate change and human activities, the regional hydrological cycle process has undergone significant changes (He *et al.* 2019; Omer *et al.* 2020). Abnormal changes in precipitation are significant, resulting in frequent regional/urban droughts and floods, which have a profound impact on regional/urban water resources development and utilization, urban water supply, production, living, and ecological environment (Pathak *et al.* 2016). With the development of society and the economy, the scale of the city continues to expand, and urban water safety has become a hot topic of public concern. Urban water security mainly includes water supply, flooding, and other aspects. Under the background of climate change and high urbanization, extreme events occur frequently, resulting in a reduction in the amount of water resources available for human control and an increase in the spatial and temporal differences in water resources (Coffel *et al.* 2019). At the same time, the seasonal distribution and amount of precipitation are key factors affecting urban water supply. Extreme precipitation, such as the maximum daily precipitation, is a key factor affecting urban floods. Therefore, analyzing the spatiotemporal variation characteristics of characteristic precipitation in a certain region has become a hot topic for scholars.

Domestic and foreign research on the spatiotemporal evolution of precipitation mainly focuses on large-scale river basins and economically developed large cities or urban agglomerations. For example, Silva Dias *et al.* (2012) used daily rainfall data in Sao Paulo, Brazil to analyze its precipitation trends. The results showed that precipitation in this region showed significant increasing trends. Caloiero (2013) found different results between the North Island and the South Island of New Zealand, where rainfall is most concentrated, with precipitation concentration on the eastern side of the South Island being comparable to that of the North Island, while precipitation concentration on the west side is the lowest. Royé & Martin-Vide (2017) studied the concentration of precipitation days in the United States and found that the less annual precipitation, the more concentrated the precipitation days are. Zhang *et al.* (2023) found that the overall winter precipitation on the Qinghai-Tibet Plateau mainly increased at a large scale, with the largest increase rate in the central and southern regions. Wang *et al.* (2023) analyzed the spatiotemporal variation characteristics of precipitation in the Jianghuai region and found that annual and summer precipitation showed an insignificant increasing trend, and spring and autumn precipitation showed

an insignificant decreasing trend. Shifteh Some'e *et al.* (2012) examined the trend of precipitation in Iran using the MK method and estimated the magnitude of the precipitation trend using the Theil-Sen slope and found that there is a significant increase in summer precipitation in Iran and an increase in the concentration of precipitation. In terms of spatial changes in precipitation, Chen & Zhang (2012) analyzed the precipitation changes at stations in the Hanjiang Basin and found that the changes in precipitation were spatially non-consistent with a decrease in precipitation in the upper reaches and an increase in precipitation in the lower reaches. Deng *et al.* (2018) used empirical orthogonal function (EOF) decomposition to study the precipitation changes in the Hanjiang Basin and found that precipitation increased in the southwestern and downstream areas of the basin, which further led to the conclusion that the spatial changes in precipitation in the Hanjiang basin are non-consistent from mathematical methods. From the above analysis, it is found that in the context of climate change, precipitation in different regions has changed significantly, mainly in the form of an increase in the concentration of precipitation on the time scale and an increase in the heterogeneity of the temporal distribution of precipitation within the year. On the spatial scale, the spatial variation of precipitation is non-consistent.

As the urbanization process continues to advance, corresponding research on precipitation in urbanized areas has gradually increased. Changnon *et al.* (1976) initiated and implemented the Metropolitan Meteorological Observation Experimental Program. The observation results showed that urbanization increased urban downwind precipitation relative to the background area. At the same time, in a study on summer precipitation changes in St. Louis, it was found that urbanization caused. There was a significant increase in rainfall downwind of the city (Changnon 1979). Seino *et al.* (2018) studied the precipitation characteristics of Tokyo and found that the heat island effect caused by urbanization will cause precipitation in urban Tokyo to increase by about 10%. In a case study of Houston, Shepherd *et al.* (2010) found that urban expansion induced a rainfall enhancement effect. Zhang (2020) found that the frequency and intensity of extreme precipitation events in urbanized areas in southeastern China showed a significant increasing trend. Han *et al.* (2015) discussed the changing characteristics of extreme precipitation in the Yangtze River Delta urban agglomeration and believed that the frequency of floods in key cities in the region was increasing. Li *et al.* (2021) analyzed the characteristics of extreme precipitation in the Guangdong-Hong Kong-Macao Bay Area and concluded that extreme precipitation in this area has increased significantly. Ding *et al.* (2019) compared the difference in precipitation during the rainy season between urban and suburban areas of Beijing and found that although precipitation during the rainy season showed a decreasing trend, urbanization still has the effect of increasing rainfall. Kang *et al.* (2021) found that urbanization in the Taihu Basin leads to an increase in extreme precipitation. Zhao *et al.* (2021) analyzed the impact of urbanization on temperature and precipitation in Shenzhen from 1979 to 2017, showing that there is a significant rain island effect in Shenzhen.

In summary, it is found that previous studies on the effect of urbanization on increasing rainfall have focused on qualitative analysis and lacked quantitative research, while the spatial scale of the relevant studies has focused on urban agglomerations and provincial-level administrative districts, and lacked quantitative research on the individual city. Shenzhen is located on the southern of Guangdong Province, the east coast of the Pearl River Delta. It is a window for China's reform and opening up, a national economic center city of China, and an international city. After more than 40 years of rapid urbanization, Shenzhen has become one of the most urbanized areas in China. Under the background of high urbanization, precipitation characteristics in Shenzhen have also undergone certain changes. Therefore, this article analyzes the spatiotemporal changes in precipitation in Shenzhen and the impact of urbanization based on Shenzhen rainfall station data. In this study, the trend-free pre-whitening MK (TFPW-MK), empirical orthogonal function, and suburban site classification are used to analyze the spatial and temporal patterns of precipitation changes in Shenzhen and the impact of urbanization on precipitation. An in-depth study of precipitation changes at different scales in Shenzhen has important practical significance for Shenzhen's water resources management, water security strategy, and flood control. Meanwhile, this study may provide a research example to study the urbanization effect of precipitation in related highly urbanized cities.

2. STUDY AREA AND METHODS

2.1. Study area

Shenzhen is located on the southern of Guangdong Province, the east coast of the Pearl River Delta. (113°43′ ~ 114°38′E, 22°24′ ~ 22°52′N). It is one of the four central cities in the Guangdong-Hong Kong-Macao Greater Bay Area. Shenzhen has a subtropical monsoon climate, with long summers and short winters, a mild climate, sufficient sunshine, and abundant rainfall. The average annual precipitation is 1,830 mm. The distribution of precipitation time is uneven. During the rainy

season (the rainy season in Shenzhen is from April to October), the multi-year average precipitation is 1,633.62 mm, which is about 85% of the annual precipitation. The city covers an area of 1,997.47 km^2, with complex terrain and diverse landform types. The terrain gradually decreases from southeast to northwest. As of 2020, the city's built-up area is 927.96 km^2. As a typical representative of rapid urbanization, Shenzhen has experienced rapid economic development, sudden population increase, and large-scale urban expansion. The city's surface coverage has changed tremendously, and the urban climate has gradually changed.

2.2. Data sources

Daily precipitation data from 10 rainfall stations in Shenzhen from 1960 to 2019 were collected. The data are all from the *Pearl River Basin Hydrological Yearbook*. The distribution of rainfall stations is shown in Figure 1. The relevant data has undergone strict quality control and is consistent, reliable, and representative. The average precipitation in Shenzhen is calculated using the Thiessen polygon method. Based on the daily rainfall data of rainfall stations, the total precipitation on wet days (PRCPTOT), precipitation intensity (SDII), rainfall of rainy season (RRS), the maximum daily precipitation per year (RX1day), the annual maximum 3-day precipitation (RX3day), the annual maximum 7-day precipitation (RX7day) of each station and area in Shenzhen are calculated. The meanings of each precipitation indicator are shown in Table 1. To analyze the impact of urbanization on precipitation in Shenzhen, sites were screened based on land use data. Land use data of Shenzhen City from 1980 to 2020 was collected. The land use remote sensing monitoring data used in the article is from the Resource and Environment Science Data Center of the Chinese Academy of Sciences (http://www.resdc.cn), with a spatial resolution of 30 m.

2.3. Trend test method

The TFPW-MK test method based on preset whitening processing is used to conduct trend tests on the precipitation indicators series in Shenzhen. This method can effectively overcome the shortcomings of the Mann–Kendall (M–K) test

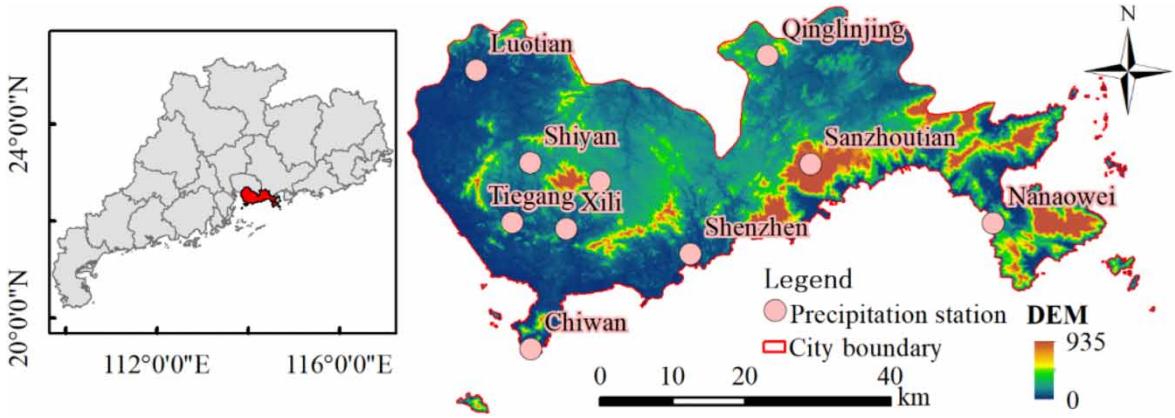

Figure 1 | Overview of Shenzhen City and distribution of rainfall stations.

Table 1 | Shenzhen precipitation indicators and their connotation

Name	Abbreviation	Connotation	Unit
Total precipitation on wet days	PRCPTOT	≥1 mm daily accumulation of precipitation	mm
precipitation intensity	SDII	The ratio of annual precipitation to number of precipitation days (daily precipitation ≥ 1 mm)	mm/d
Rainfall during the rainy season	RRS	Precipitation from April to October	mm
Maximum precipitation in 1 day	RX1day	Maximum daily precipitation per year	mm
Maximum precipitation in 3 days	RX3day	The annual maximum 3-day precipitation	mm
Maximum precipitation in 7 days	RX7day	The annual maximum 7-day precipitation	mm

method that leads to inaccurate analysis results due to autocorrelation (Gebru *et al.* 2022). The specific calculation steps of TFPW-MK are as follows:

Assume that the trend term T_t in the original data sequence X_t is linear, remove the trend term of the sequence X_t to obtain the sequence Y_t:

$$Y_t = X_t - T_t = X_t - \beta \cdot t \quad \beta = \text{Median}(\frac{x_j - x_i}{j - i}) \tag{1}$$

Second, calculate the first-order autocorrelation coefficient of the sequence Y_t:

$$r_1 = \frac{\sum_{t=1}^{n-1}(x_t - \overline{x_t})(x_{t+1} - \overline{x_{t+1}})}{\sqrt{\sum_{t=1}^{n-1}(x_t - \overline{x_t})^2 \sum_{t=1}^{n-1}(x_{t+1} - \overline{x_{t+1}})}} \tag{2}$$

Conduct a significance test on the first-order autocorrelation coefficient r_1. If it fails the significance test, the Y_t sequence is considered independent. The original sequence X_t can be directly tested using the M–K method. Otherwise, it is necessary to use the preset blank method to remove the autocorrelation terms in the sequence and construct an independent sequence Y_t':

$$Y_t' = Y_t - r_1 \cdot Y_{t-1} \tag{3}$$

Finally, the trend term T_t is merged with the independent sequence Y_t' to obtain a new sequence Y_t'', and the obtained new sequence Y_t'' is used to perform the M–K test. For details on the M–K test method, please refer to the references (Güçlü 2020).

2.4. Spatial modal analysis

EOF is a commonly used method for spatial distribution mode analysis. It is a method for analyzing the structural characteristics of matrix data and extracting main data features. It is widely used in meteorological and climate research. Concentrate the information of the original multiple variables to the maximum extent on the principal components of a few independent variables. The greater the cumulative variance contribution rate of the principal components, the greater the information the principal component accounts for in the original variables. EOF can reflect the spatial distribution characteristics of the element field to a certain extent (Eom *et al.* 2017). The specific algorithm is as follows:

(1) Preprocess the original data of m spatial fields with a time scale of n into an anomaly form to obtain a data matrix $X_{m\times n}$.
(2) Calculate the cross product of matrix X and its transposed matrix X^T to obtain the square matrix $C_{m\times m}$:

$$C_{m\times m} = \frac{1}{n} X \times X^T \tag{4}$$

(3) Calculate the characteristic roots ($\lambda_1, \lambda_2, \lambda_3, \ldots, \lambda_n$) and eigenvector $V_{m\times m}$ of the square matrix C, both of which satisfy:

$$C_{m\times m} \times V_{m\times m} = V_{m\times m} \times E_{m\times m} \tag{5}$$

where E is an m-dimensional diagonal matrix. The above characteristic roots λ are all greater than 0, and$\lambda_1 > \lambda_2 > \lambda_3 > \ldots > \lambda_n$. The eigenvector corresponding to each characteristic root is an EOF mode. For example, λ_1 corresponds to the first main mode of the original data.

(4) *Calculate time coefficients*: Project EOF onto the original data matrix to obtain the time coefficients corresponding to all spatial vectors. The calculation formula is as follows:

$$PC_{m\times n} = V_{m\times m}^T \times V_{m\times m} \tag{6}$$

Each row of data in the matrix $PC_{m\times n}$ is the time coefficient of the corresponding feature vector.

(5) *Calculation contribution rate*: the variance size of matrix X can be simply expressed by the numerical value of the characteristic root. The higher theλ, the more important the corresponding mode is and the greater the contribution to the total

variance. The contribution rate of the total variance corresponding to the *i*th mode is as follows:

$$\frac{\lambda_i}{\sum_{k=1}^{m} \lambda_k} \times 100\% \tag{7}$$

(6) *Significance test*: The decomposed EOF needs to be tested for significance. Generally, it needs to pass the North criterion. The characteristic root error at the 95% level:

$$e_i = \lambda_i \sqrt{\frac{2}{N}} \tag{8}$$

In the formula: λ_i is the eigenvector value. N is the effective degree of freedom of the sample. When adjacent eigenvalues are satisfied $\lambda_i - \lambda_{i+1} \geq e_i$, the EOF values corresponding to the two eigenvalues are considered to be valuable signals.

3. RESULTS AND DISCUSSION

3.1. Precipitation time course changes in Shenzhen

A trend test was conducted on the precipitation at 10 rainfall stations in Shenzhen. Figure 2 reflects the changing trends and spatial differences of different precipitation indicators in Shenzhen from 1960 to 2019. From the results, PRCPTOT and RRS showed an insignificant upward trend at all stations in Shenzhen. For SDII, 6 of the 10 rainfall stations in Shenzhen showed a downward trend, among which Xili Reservoir Station and Sanzhoutian Reservoir Station showed a significant decrease, and 4 stations showed an upward trend, mainly located in the west of Shenzhen City, among which Shenzhen Reservoir Station showed a significant upward trend. In Shenzhen, 7 sites on RX1day showed a downward trend, 5 sites on RX3day showed a downward trend, and 4 sites on RX7day showed a downward trend. Most of the sites were located in the southwest of Shenzhen, and the remaining sites with an upward trend were located in the northeast of Shenzhen.

To further analyze the changes in precipitation in Shenzhen, Table 2 gives the statistical values of the characteristic elements of the average precipitation in Shenzhen from 1960 to 2019. Figures 3 and 4, respectively, show the changes in the average precipitation indicators and the M–K statistic change curve in Shenzhen. It can be seen from Table 2 that the climate tendency rate, M–K statistic z-value and Sen's slope calculation results of PRCPTOT, SDII, RRS, RX1day, RX3day, and RX7day are 42.56 mm/10a, 1.34, 2.96; −0.2 mm/d/10a −0.88, −0.02; 33.72 mm/10a, 1.61, 2.96; 1.96 mm/10a, 0.19, −0.12; 0.74 mm/10a, 0.09, −0.06; 2.72 mm/10a, 0.40, 0.18; respectively. All indicators failed the 0.05 significance test, the trend was not significant, and only SDII showed a downward trend.

From Figure 3, the change patterns of the precipitation indicators in Shenzhen are consistent with the stations, and the precipitation indicators in Shenzhen have obvious oscillation periods, and the oscillation period is about 10–20 years (Fu

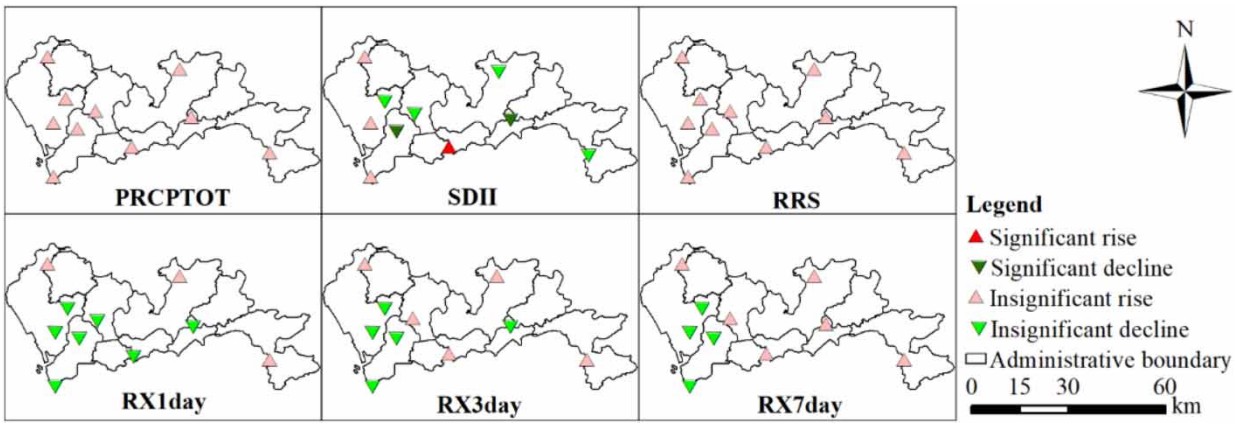

Figure 2 | Results of the change trend test of precipitation indicators at various stations in Shenzhen City.

Table 2 | Statistical value of average extreme precipitation indicators in Shenzhen

	Propensity rate (mm/10a)	TFPW-MK value	β	Trend
PRCPTOT	42.56	1.34	2.96	↑
SDII	−0.20	−0.88	−0.02	↓
RRS	33.72	1.61	2.96	↑
RX1day	1.96	0.19	−0.12	↑
RX3day	0.74	0.09	−0.06	↑
RX7day	2.72	0.40	0.18	↑

Note: The significance level is 0.05, '↓' indicates a downward trend, and '↑' indicates an upward trend.

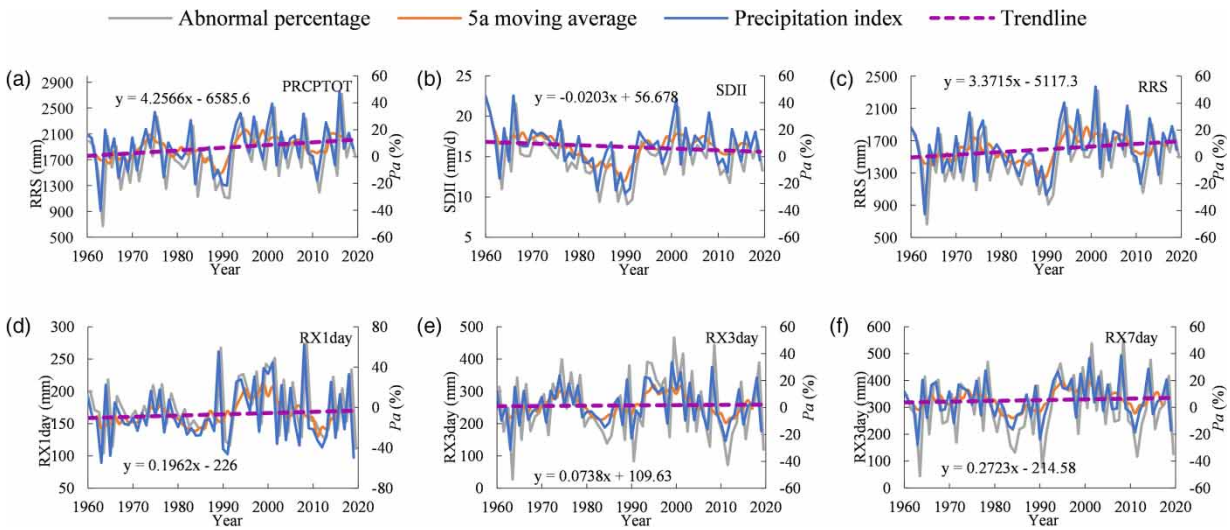

Figure 3 | Interannual variations of regional average extreme precipitation indicators.

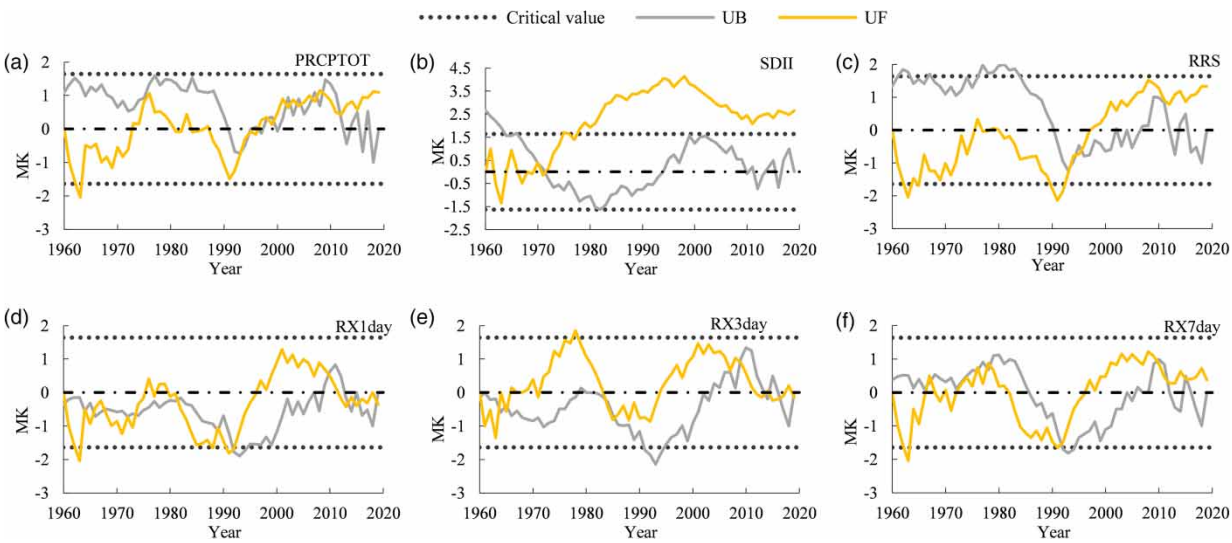

Figure 4 | TFPW-MK trend test results of regional average precipitation indicators.

et al. 2022). Although there are fluctuations, except for SDII, the rest of the Shenzhen precipitation indicators show an overall upward trend. From the results of the M–K mutation test of the precipitation indicators (Figure 4), it can be seen that for SDII, the intersection of the UF statistic sequence and the UB statistic sequence appeared in 1972, indicating that the precipitation intensity mutated during this period. For the four indicators PRCPTOT, RRS, RX1day, and RX7day, the UF and UB curves had multiple intersection points between 1960 and 2019. However, after 1991, the UF and UB curves had intersection points and their relative positions changed. It shows that significant mutations occurred in PRCPTOT, RRS, RX1day, and RX7day in Shenzhen City in 1991. Combined with Figure 3, it can be found that precipitation changed from a year-by-year decrease before 1991 to a year-by-year increase trend after 1991.

3.2. Spatial variation characteristics of precipitation in Shenzhen

Taking into account the physical meaning of different precipitation indicators, the EOF method is used to decompose the RRS and RX7day indicators in Shenzhen. Among them, RRS reflects the changing characteristics of long-duration precipitation in Shenzhen, and RX7day can reflect the distribution characteristics of short-duration heavy rains in Shenzhen. The cumulative variance contribution of RRS and RX7day eigenvectors is shown in Table 3. It can be seen from Table 3 that the precipitation fields corresponding to RRS and RX7day converge quickly. The cumulative variance contribution rates of the first two principal components account for 77.6 and 64.3%, respectively. Both of them passed the North criterion significance test. Therefore, the distribution modes of the first two principal components can characterize the variability distribution structure of the precipitation variable field in Shenzhen.

Figure 5 shows the spatial distribution modes and time coefficients of the first two principal components of the EOF decomposition of the two precipitation indicators RRS and RX7day. As can be seen from Figure 5, the precipitation amounts corresponding to RRS and RX7day have similar distribution characteristics in the first two main modes. Affected by meteorological conditions, the two precipitation indicators roughly show two types of distribution modes. The variance contribution rates of the eigenvectors of mode 1 are 66.4 and 48.4%, respectively, which are much higher than the contribution rates of other modes and can be considered the most important spatial distribution pattern of precipitation fields in Shenzhen. It can be seen from the figure that the eigenvalues of the first mode of RRS and RX7day are both positive, indicating that the changing trend of annual precipitation in Shenzhen from 1960 to 2019 is consistent. That is, either all of them show an increasing trend or all of them show a decreasing trend. The precipitation center is located near Nan'aowei in the Dapeng Bay District in the southeast, indicating large precipitation changes in this area. The low-value center is located near Luotian and Qinglinjing in the northwest, indicating that precipitation changes in this area are small. From the perspective of time coefficients, the time coefficients of RRS and RX7day were mostly negative before 1990, indicating that the precipitation center in Shenzhen during this period was concentrated in the northwest. After 1990, the time coefficient is mostly positive, indicating that the southeast is the precipitation center of Shenzhen City.

The variance contribution rates of the second main mode eigenvectors of RRS and RX7day are 11.2 and 15.9%, respectively. The distribution is roughly divided between Shenzhen Reservoir Station and Qinglinjing Station. The eigenvector

Table 3 | Cumulative variance contribution rate of the top five eigenvectors of EOF decomposition of two precipitation indicators

Extreme precipitation indicator	Mode	Eigenvector value	Variance contribution rate (%)	Cumulative variance contribution rate (%)	$\lambda_i - \lambda_{i+1}$	e_i
RRS	1	571741.3	66.4	66.4	475071.7	255690.5
	2	96669.6	11.2	77.6	44401.6	43232.0
	3	52268.0	6.1	83.6	7557.9	23375.0
	4	44710.2	5.2	88.8	18550.5	19995.0
	5	26159.7	3.0	91.9	3596.1	11699.0
RX7day	1	38440.0	48.4	48.4	25839.7	16390.9
	2	12600.3	15.9	64.3	5482.5	5372.8
	3	7117.8	9.0	73.3	594.1	3035.4
	4	6523.7	8.2	81.5	2318.4	2781.7
	5	4205.3	8.3	86.8	826.2	1793.1

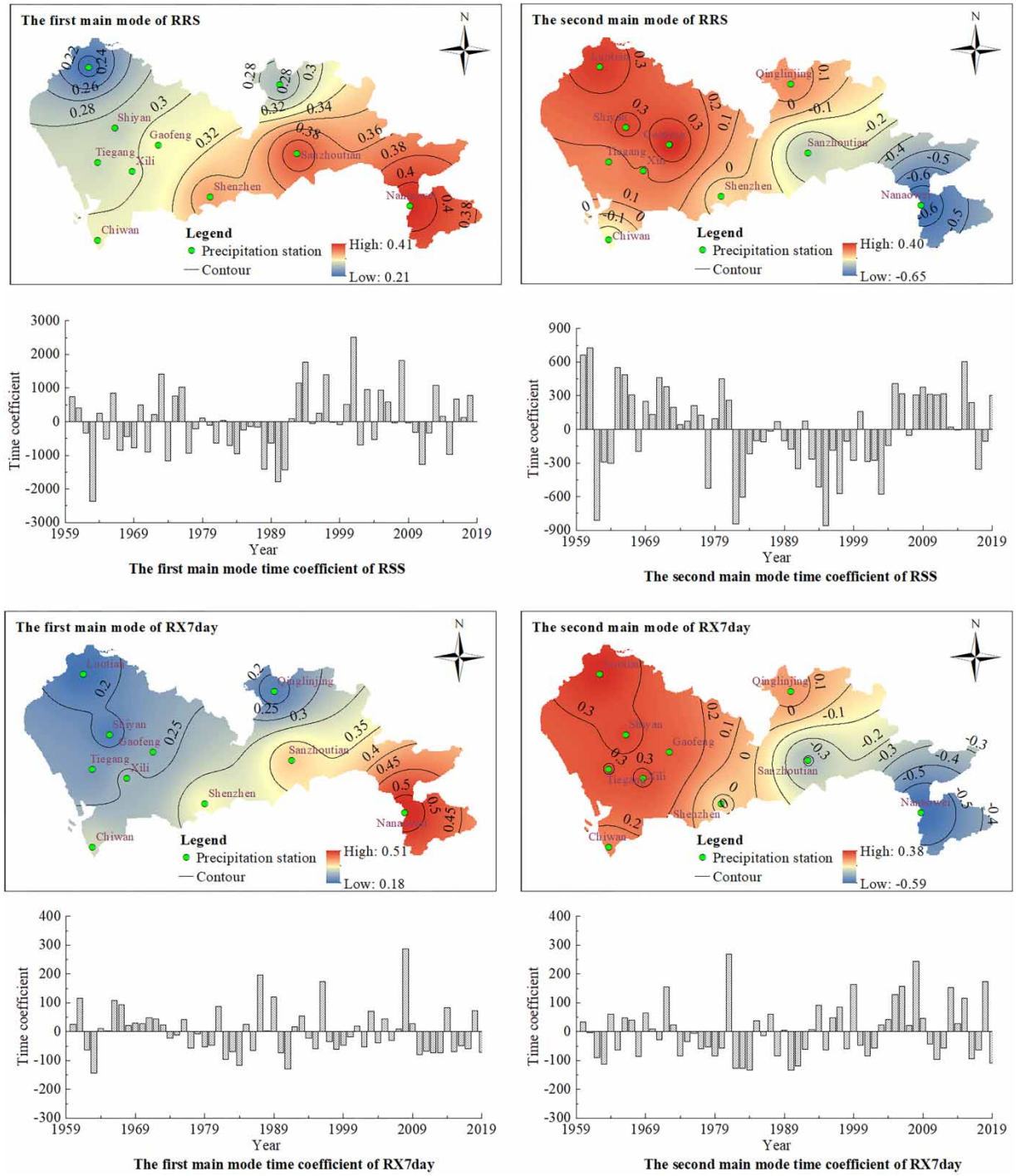

Figure 5 | Spatial distribution modes and time coefficients of the first two principal components of EOF decomposition of RRS and RX7day.

has negative values to the east and positive values to the west. The positive value center appears near Gaofeng and Luotian in the northwest, and the negative value center appears near Nan'aowei in the Dapeng Bay District in the southeast, showing an 'East-West' reverse distribution characteristic. This shows that Shenzhen has a spatial distribution of floods in the west and drought in the east or drought in the west and floods in the east. The time coefficients of the second main mode of RRS and RX7day over the years show that under this mode, rainfall in the east and west changes alternately with high and low rainfall, and has certain periodic characteristics.

3.3. The impact of urbanization on precipitation in Shenzhen

The rainfall stations were divided into urban and suburban stations based on Shenzhen socioeconomic data and land use data (Wang *et al.* 2021). Shenzhen Reservoir Station was selected as an urban station and Sanzhoutian Station was selected as a suburban station (Table 4). The differences in the evolution of precipitation indicators in urban and suburban areas were analyzed from two perspectives: a long series comparison of extreme precipitation indicators between urban and suburban rainfall stations and a comparison at different development stages.

3.3.1. Comparison of series of precipitation indicators between urban and suburban meteorological observation stations

Figure 6 shows the change process of precipitation indicators at urban and suburban rainfall stations in Shenzhen. It can be seen from Figure 6(a), and (c) that the changes in annual precipitation and flood season precipitation in urban and suburban areas of Shenzhen show an increasing trend, but there is a slight difference in the degree of increase. The linear increases in annual precipitation in urban areas and flood season precipitation are relatively large. Among them, the linear increases of PRCPTOT in urban stations and suburban stations are 51.69 and 26.16 mm/10a, respectively, and for RRS, the linear increases in urban stations and suburban stations are 49.78 and 22.22 mm/10a, respectively. From Figure 6(b), (d)–(f), the changing trends of SDII, RX1day, RX3day, and RX7day are opposite for urban stations and suburban stations. The above indicators of suburban stations show a downward trend, while those of urban stations show an upward trend. From the perspective of change amplitude, the differences of SDII, RX1day, RX3day, and RX7day in suburban stations showed an increasing trend at the rates of 0.136, 0.282, 0.380, and 0.328 mm/a, respectively. In general, before 2000, PRCPTOT, SDII, RRS, RX1day, RX3day, and RX7day in the suburbs of Shenzhen were higher than the corresponding precipitation indicators in the urban area. However, in recent years, there has been a tendency for the precipitation indicators in suburban stations to be smaller than those in urban areas. Based on the above analysis, it is found that the urbanization process in Shenzhen has a significant impact on different precipitation indicators in Shenzhen, and has a certain rainfall-enhancing effect, especially the extreme precipitation indicators.

Table 4 | Classification of urban and suburban meteorological stations

Rainfall station	Proportion of artificial construction area (%)	Absolute altitude (m)	Type
Shenzhen reservoir station	92.4	44.0	Urban station
Sanzhoutian station	21.6	50.0	Suburban station

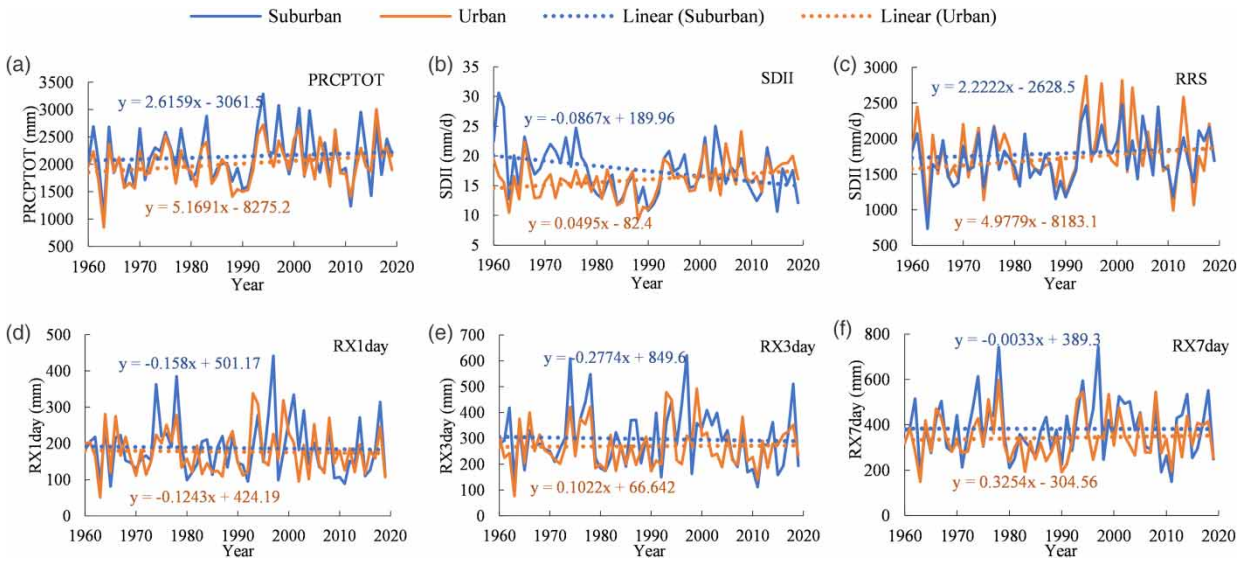

Figure 6 | Variation processes of extreme precipitation at urban and suburban meteorological stations.

Table 5 | Comparison of extreme precipitation between urban sites and suburban sites in different stages

	1960–1991 average (mm)			1991–2019 average (mm)			Amplitude (%)		
	Urban	Suburban	Differences	Urban	Suburban	Differences	Urban	Suburban	Differences
PRCPTOT	1899.0	2056.7	−157.7	2126.1	2234.8	−108.7	11.96	8.66	−31.06
SDII	16.1	18.7	−2.6	16.0	18.3	−2.3	−0.66	−2.02	−10.4
RRS	1695.5	1453.4	242.0	1896.4	1613.2	283.2	11.85	10.99	17.00
RX1day	172.9	185.5	−12.6	181.0	188.5	−7.4	4.72	1.59	−41.27
RX3day	262.1	292.0	−30.1	278.6	303.9	−25.3	6.30	4.07	−15.44
RX7day	328.1	368.7	−40.7	358.5	397.8	−39.2	9.29	7.88	−3.52

3.3.2. Comparison of extreme precipitation indicators at different stages in urban and suburban meteorological observation stations

Shenzhen's urbanization is mainly divided into two obvious stages. The main turning point is 1991. Based on previous research, the first main cycle of annual precipitation in the study area is about 10, the main mutation year is 1991, and there is a 60-year annual precipitation sequence from 1960 to 2019. Therefore, the 60-year precipitation series in Shenzhen can be divided into two periods with 1991 as the boundary. The lengths of the two periods before and after are 31a and 29a, respectively. The two periods happen to be roughly 3 periods, which can avoid the influence of the periodic sequence on the precipitation change results due to the random selection of periods.

Taking 1991 as the dividing point, the precipitation changes in Shenzhen at different urbanization stages were studied. Table 5 shows the comparison of precipitation indicators between urban and suburban stations in Shenzhen at different stages. It can be seen from Table 5 that for PRCPTOT, the precipitation difference between urban and suburban areas in Shenzhen develops in a decreasing trend. A longitudinal comparison of urban and suburban areas in different periods shows that the average precipitation in the urban area from 1991 to 2019 increased by 11.96% compared with the average precipitation from 1960 to 1990, while the annual precipitation in the suburbs increased by 8.66% in the two periods. In terms of average annual precipitation, the difference between the annual precipitation in the suburbs and the urban area from 1960 to 1990 was 157.67 mm. From 1991 to 2019, the difference narrowed to 108.69 mm, a decrease of 31.06%. In terms of SDII, precipitation intensity in both urban and suburban areas decreased after 1991, but the decrease in suburban areas was greater, at −2.02%. The RRS in urban areas and suburbs from 1991 to 2019 increased by 11.58 and 10.99%, respectively, compared with before 1991. The RRS of urban stations is larger than that of suburban stations. With the development of urbanization, the urban–suburban difference in rainfall during flood season in Shenzhen has also expanded from 242.0 mm before 1991 to 283.14 mm. In terms of extreme precipitation, in the past 60 years, the extreme precipitation in Shenzhen's suburbs was much greater than that in urban stations. Before 1991, the differences in RX1day, RX3day, and RX7day between suburban stations and urban stations were 12.6, 30.1, and 40.7 mm, respectively. After 1991, the value shrank to 7.4, 25.3, and 39.2 mm.

The above analysis shows that except for RRS, the PRCPTOT, SDII, RX1day, RX3day, and RX7day of urban stations in Shenzhen are smaller than those of suburban stations. However, with the development of urbanization, the differences between urban and suburban stations are decreasing. The RRS of urban areas is larger than that of suburban stations, and the difference is constantly expanding, indicating that urbanization in Shenzhen has a certain rainfall-enhancing effect on various precipitation indicators. In terms of extreme precipitation, the smaller the precipitation scale, the stronger the rainfall-enhancing effect of urbanization.

4. CONCLUSION

(a) Shenzhen's PRCPTOT, RRS, RX1day, RX3day, and RX7day all showed an insignificant upward trend. SDII showed an insignificant decreasing trend. Except for PRCPTOT and RRS, the changing trends of other indicators have certain spatial heterogeneity. Among them, some stations showed a downward trend in terms of extreme precipitation, and they were mainly located in the west of Shenzhen City.

(b) Shenzhen's precipitation indicators all have obvious oscillation periods, and the oscillation period is about 10–20 years. Shenzhen's SDII mutated in 1972; the four precipitation indicators PRCPTOT, RRS, RX1day, and RX7day mutated in 1991. The corresponding precipitation changed from a yearly decrease before 1991 to a yearly increase after 1991.

(c) Different precipitation indicators in Shenzhen have similar distribution modes. The first main mode shows global consistency, showing that the precipitation in Shenzhen is either rainy or less rainy, and reflects that the precipitation center of Shenzhen has changed from the northwest before 1990 to the southeast after 1990. The second main mode shows an 'East-West' reverse distribution, that is, precipitation increases in the east and decreases in the west, or precipitation increases in the west and decreases in the east.

(d) Urbanization has a significant impact on the spatial distribution of precipitation in Shenzhen and has an increasing effect on the city's PRCPTOT, RRS, and extreme precipitation. The impact of urbanization on extreme precipitation on smaller time scales is more severe, making cities more vulnerable to the risk of extreme floods.

DATA AVAILABILITY STATEMENT

All relevant data are available from https://github.com/ssw16/-.git.

CONFLICT OF INTEREST

The authors declare there is no conflict.

REFERENCES

Caloiero, T. 2013 Analysis of daily rainfall concentration in New Zealand. *Nat. Hazards* **72**, 389–404.

Changnon Jr., S. A. 1979 Rainfall changes in summer caused by St. Louis. *Science* **205**, 402–404.

Changnon, S. A., Semonin, R. G. & Huff, A. F. 1976 A hypothesis for urban rainfall anomalies. *J. Appl. Meteorol.* **15**, 544–560.

Chen, Y. & Zhang, X. 2012 Long-term variation trend and sustainability analysis of precipitation, evaporation and runoff in Hanjiang Basin. *Water Resour. Power* **30** (6), 6–8.

Coffel, E. D., Keith, B., Lesk, C., Hroton, R. M., Bower, E., Lee, J. & Mankin, J. S. 2019 Future hot and dry years worsen Nile basin water scarcity despite projected precipitation increases. *Earth's Future* **7**, 967–977.

Deng, P., Bing, J., Jia, J. & Wang, D. 2018 Pattern of spatio-temporal variability of flood season precipitation in Hanjiang River Basin between 1956 and 2016. *Yangtze Resour. Environ.* **27** (09), 2132–2141.

Ding, K., Zhang, L., Song, X., She, D. X. & Jun, X. 2019 Temporal and spatial features of precipitation and impact of urbanization on precipitation characteristics in flood season in Beijing. *Geogra. Prog.* **38** (12), 1917–1932.

Eom, J., Seo, K.-W. & Ryu, D. 2017 Estimation of Amazon River discharge based on EOF analysis of GRACE gravity data. *Remote Sens. Environ.* **191**, 55–66.

Fu, Y., Xu, Z., Chen, H., Huang, Y. & Ye, C. 2022 Analysis on spatiotemporal evolution characteristics of precipitation in Guangdong-Hong Kong-Macao Greater Bay Area from 1961 to 2014. *Water Resour. Prot.* **38** (04), 56–65. + 74.

Gebru, B. M., Adane, G. B., Park, E., Khamzina, A. & Lee, W.-K. 2022 Landscape pattern and climate dynamics effects on ecohydrology and implications for runoff management: Case of a dry Afromontane forest in northern Ethiopia. *Geocarto Int.* **37**, 12466–12487.

GüçLü, Y. S. 2020 Improved visualization for trend analysis by comparing with classical Mann–Kendall test and ITA. *J. Hydrol.* **584**, 124674.

Han, L., Xu, Y., Pan, G., Deng, X., Hu, C., Xu, H. & Shi, H. 2015 Changing properties of precipitation extremes in the urban areas, Yangtze River Delta, China, during, 1957–2013. *Nat. Hazards* **79**, 437–454.

He, Y., Qiu, H., Song, J., Zhao, Y., Zhang, L., Hu, S. & Hu, Y. 2019 Quantitative contribution of climate change and human activities to runoff changes in the Bahe River watershed of the Qinling Mountains, China. *Sustainable Cities Soc.* **51**, 101729.

Kang, C., Luo, Z., Zong, W. & Hua, J. 2021 Impacts of urbanization on variations of extreme precipitation over the Yangtze River Delta. *Water-sui* **13**, 150.

Li, Y., Wang, W., Chang, M. & Wang, X. 2021 Impacts of urbanization on extreme precipitation in the Guangdong-Hong Kong-Macau Greater Bay Area. *Urban Clim.* **38**, 100904.

Omer, A., Elagib, N. A., Zhuguo, M., Saleem, F. & Mohammed, A. 2020 Water scarcity in the Yellow River Basin under future climate change and human activities. *Sci. Total Environ.* **749**, 141446.

Pathak, P., Kalra, A. & Ahmad, S. 2016 Temperature and precipitation changes in the Midwestern United States: Implications for water management. *Int. J. Water Resour. Dev.* **33**, 1003–1019.

Royé, D. & Martin-vide, J. 2017 Concentration of daily precipitation in the contiguous United States. *Atmos. Res.* **196**, 237–247.

Seino, N., Aoyagi, T. & Tsuguti, H. 2018 Numerical simulation of urban impact on precipitation in Tokyo: How does urban temperature rise affect precipitation? *Urban Clim.* **23**, 8–35.

Shepherd, J. M., Carter, M., Manyin, M., Messen, D. & Burian, S. 2010 The impact of urbanization on current and future coastal precipitation: A case study for Houston. *Environ. Plan. B: Plann. Des.* **37**, 284–304.

Shifteh Some'e, B., Ezani, A. & Tabari, H. 2012 Spatiotemporal trends and change point of precipitation in Iran. *Atmos. Res* **113**, 1–12.

Silva dias, M. A. F., Dias, J., Carvalho, L. M. V., Freitas, E. D. & Silva dias, P. L. 2012 Changes in extreme daily rainfall for São Paulo, Brazil. *Clim. Change* **116**, 705–722.

Wang, H., Wu, W., Wang, G., Zhao, Z., Chen, J. & Yan, C. 2021 Evolution characteristics of extreme precipitation events and its urban effect in Kunming City. *Water Resour. Prot.* **37** (04), 61–68.

Wang, Y., Wu, H., Wang, P. & Peng, Z. 2023 Spatiotemporal variability of precipitation in the Jianghuai Region during 1960–2017. *Soil Water Conserv. Res.* **30** (04), 236–244. + 255.

Zhang, D. 2020 Rapid urbanization and more extreme rainfall events. *Sci. Bull.* **65**, 516–518.

Zhang, S., C, E., Li, X., Qi, D. & Zhou, L. 2023 Research on the characteristics of precipitation change and center of gravity migration in winter half year of 1960–2019 in the Qinghai Plateau. *J. Nat. Disas.* **32** (03), 118–130.

Zhao, Y., Xia, J., Xu, Z., Zou, L., Tan, Q. & Chen, H. 2021 Rain island effect in Shenzhen City. *J. Beijing Norm. Univ. (Nat. Sci.)* **57** (6), 768–775.

First received 21 March 2024; accepted in revised form 23 July 2024. Available online 2 August 2024